JACS
JOURNAL OF THE AMERICAN CHEMICAL SOCIETY
Article
pubs.acs.org/JACS

Microfluidic Mixing Triggered by an External LED Illumination

Anna Venancio-Marques,[†,‡,§] Fanny Barbaud,[†,‡,§] and Damien Baigl*[,†,‡,§]

[†]Department of Chemistry, Ecole Normale Supérieure, 24 rue Lhomond, 75005 Paris, France
[‡]Université Pierre et Marie Curie Paris 6, 4 Place Jussieu, 75005 Paris, France
[§]UMR 8640, CNRS, France

Supporting Information

ABSTRACT: The mixing of confined liquids is a central yet challenging operation in miniaturized devices. Microfluidic mixing is usually achieved with passive mixers that are robust but poorly flexible, or active mixers that offer dynamic control but mainly rely on electrical or mechanical transducers, which increase the fragility, cost, and complexity of the device. Here, we describe the first remote and reversible control of microfluidic mixing triggered by a light illumination simply provided by an external LED illumination device. The approach is based on the light-induced generation of water microdroplets acting as reversible stirrers of two continuous oil phase flows containing samples to be mixed. We demonstrate many cycles of reversible photoinduced transitions between a nonmixing behavior and full homogenization of the two oil phases. The method is cheap, portable, and adaptable to many device configurations, thus constituting an essential brick for the generation of future all-optofluidic chip.

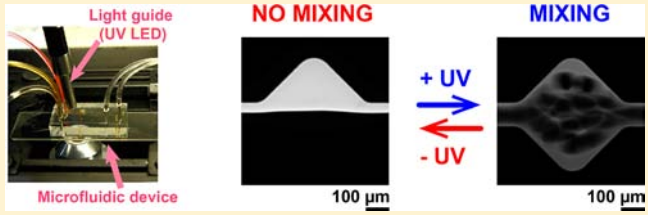

INTRODUCTION

Mixing of at least two liquids is a key-operation in most chemical and biochemical processes. In miniaturized devices, the confinement of liquids usually imposes laminar flow conditions where mixing is mainly controlled by diffusion. From the beginning of microfluidics,[1] great efforts have thus been directed at developing microfluidic mixers.[2] Passive mixers,[3−7] which rely on diffusion[8] or chaotic advection,[9−11] are robust and easy to implement but lack flexibility. Active mixers,[12−14] where mixing is triggered by an external stimulus, enable dynamic and tunable mixing, but the necessity to implement external transducers such as pumps[15,16] or electrodes[17,18] increases the complexity and fragility of the device while reducing its portability. With the development of optofluidics,[19] a new paradigm for the control of microfluidic systems has led to light-driven microfluidics, where microscale liquids are actuated with a light stimulus.[20] Although light has been demonstrated to control a variety of microfluidic operations[20] such as injection,[21] pumping,[22−26] flow rate control,[27] and droplet generation[28,29] or manipulation,[30−34] only one example of reversible mixing in a continuous flow was reported. It was achieved by generating a cavitation bubble in the flowing liquids using a highly focused nanosecond laser.[35] However, this interesting strategy required an elaborate optical setup and induced the generation of a hot plasma. It was thus necessary to look for a novel strategy to achieve the first reversible microfluidic mixing triggered by a simple and portable illumination, without heating the device nor implementing any supplemental transducer.

To allow light-triggerable mixing in microfluidic systems, we implemented a laser-free strategy relying on light-induced generation of water microdroplets to stir two continuous oil phases. Although mixing inside water-in-oil droplets has been well studied,[36−38] droplets, unlike their gas bubble counterparts,[39−42] had never been used to stir the external continuous phase. To control droplet generation with light, we injected a light-sensitive water phase between two oil phases using a flow-focusing geometry (Figure 1A). Before the trigger was applied, the continuous water phase between the two oil phases in the channel formed a three-layer flow, which prevented any mixing of the oil phases (Figure 1A, top). In response to a UV stimulus, the water phase was fragmented into water droplets in the flow-focusing region. Thanks to a series of expansion chambers distributed downstream, the droplets gained a multidirectional motion that allowed the two oil phases to mix with an efficiency that depended on the chamber position (Figure 1A, bottom). Provided that the continuous water phase can be photoreversibly fragmented into droplets, our approach allows reversible microfluidic mixing of two oil phases. To this end, we used a photosensitive azobenzene surfactant,[33,43] AzoTAB (Figure 1B), as it was recently shown that, by adding AzoTAB to the water phase, a photoreversible transition between a continuous laminar flow of water (tube regime, -UV) and a stable droplet regime (+UV) could be attained.[28] Not only is this approach free of any constraint to implement optical element inside the microfluidic device, but it also does not require any elaborate optical setup or laser source. In our experiments, we simply used a light-emitting diode (LED) working at 365 nm as an excitation source and the illumination

Received: December 8, 2012
Published: January 25, 2013

   dx.doi.org/10.1021/ja311837r | J. Am. Chem. Soc. 2013, 135, 3218−3223

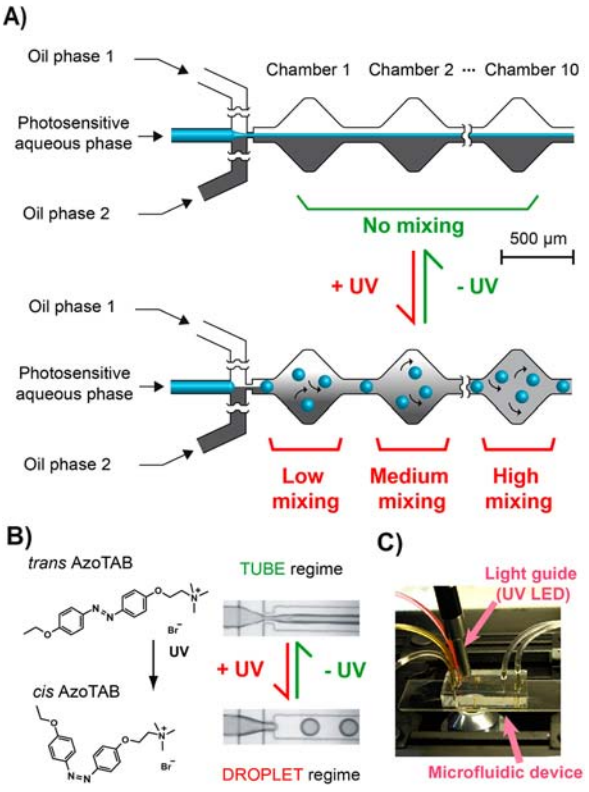

Figure 1. Concept and design of a reversible optofluidic mixer. (A) Two oil phases and a photosensitive water phase are injected in a flow-focusing device (drawn to scale) containing a series of 10 regularly spaced expansion chambers. Without UV, the system is in a stable laminar flow regime where no mixing occurs. The application of UV light induces the fragmentation of the water phase into microdroplets stirring the two oil phases to different degrees of mixing. When the UV stimulus is turned off, the system goes back to a nonmixing state. (B) The photosensitive surfactant AzoTAB undergoes a trans−cis isomerization upon illumination at 365 nm allowing to reversibly switch the water phase from a tube to a droplet generation regime by UV light. (C) The microfluidic device made of a PDMS block bonded to a glass slide (25 mm wide) is illuminated with a light guide connected to a UV LED source working at 365 nm.

was applied by placing the tip of a light guide ∼1 cm above the microfluidic device (Figure 1C).

RESULTS AND DISCUSSION

Experimental Setup. For all experiments, the microfluidic chip was made of poly(dimethylsiloxane) (PDMS) on glass, with the channel design shown in Figure 1A and a uniform channel height of 50 μm (Complete design in Figure S1). The oil phases were oleic acid with (oil phase 1) or without (oil phase 2) a fluorescent dye, Nile Red (85 μM). Under our conditions of observation, the fluorescence intensity varied linearly with Nile Red concentration (Figure S2), allowing us to monitor the mixing between the oil phases. Water phase was a 8 mM solution of AzoTAB. The oil flow rate was Q_{oil} = 0.5 μL min^{-1} for both phases and the water flow rate was Q_{water} = 2.5 - 5 μL min^{-1}.

Light-Induced Mixing. To quantify the mixing along the microfluidic device, we analyzed for each chamber the distribution of fluorescence intensity in two regions of equal area situated in the top and bottom parts (regions 1 and 2, respectively) of the device (Figure 2A). In the absence of a UV

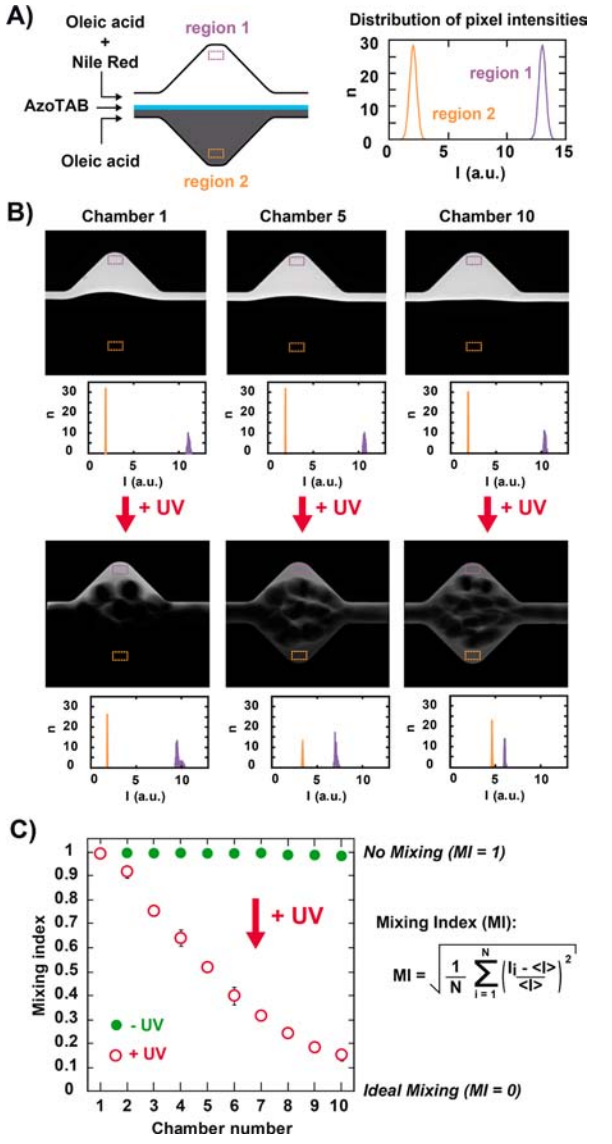

Figure 2. UV-induced mixing. (A) Nile Red (85 μM) in oleic acid, AzoTAB (8 mM) in water, and pure oleic acid are injected in the device. Distributions of pixel intensities are measured by fluorescence microscopy in two regions of equal area. (B) Representative fluorescence microscopy images (acquisition time: 10 ms) and corresponding distributions of pixel intensities in chambers 1, 5, and 10, before and after UV illumination. Each image has a size of 768 μm × 698 μm. (C) Mixing index (MI) as a function of chamber position before and after UV illumination, calculated from intensity distributions using the displayed equation where I_i is the intensity of pixel i while N and $\langle I \rangle$ are respectively the total number of pixels and average intensity over the two regions. Symbols show the mean values ± std on triplicates. Error bars smaller than symbol size are not shown. For all experiments, Q_{oil} = 0.5 μL min^{-1}, Q_{water} = 5 μL min^{-1}.

stimulus, a stable tube regime of the water phase was observed in all chambers. As a result, the oil phases 1 and 2 remained respectively highly and poorly fluorescent all along the channel (Figure 2B, top). Upon UV illumination, a stable droplet regime was rapidly observed in all chambers leading to a marked change of intensity distributions (Figure 2B, bottom). This effect was enhanced from chamber 1 to chamber 5 to chamber 10. The droplets were clearly instrumental in the mixing of the two oil phases, with an efficiency that increased along the channel (Supporting Information Movie S1). From

dx.doi.org/10.1021/ja311837r | J. Am. Chem. Soc. 2013, 135, 3218−3223

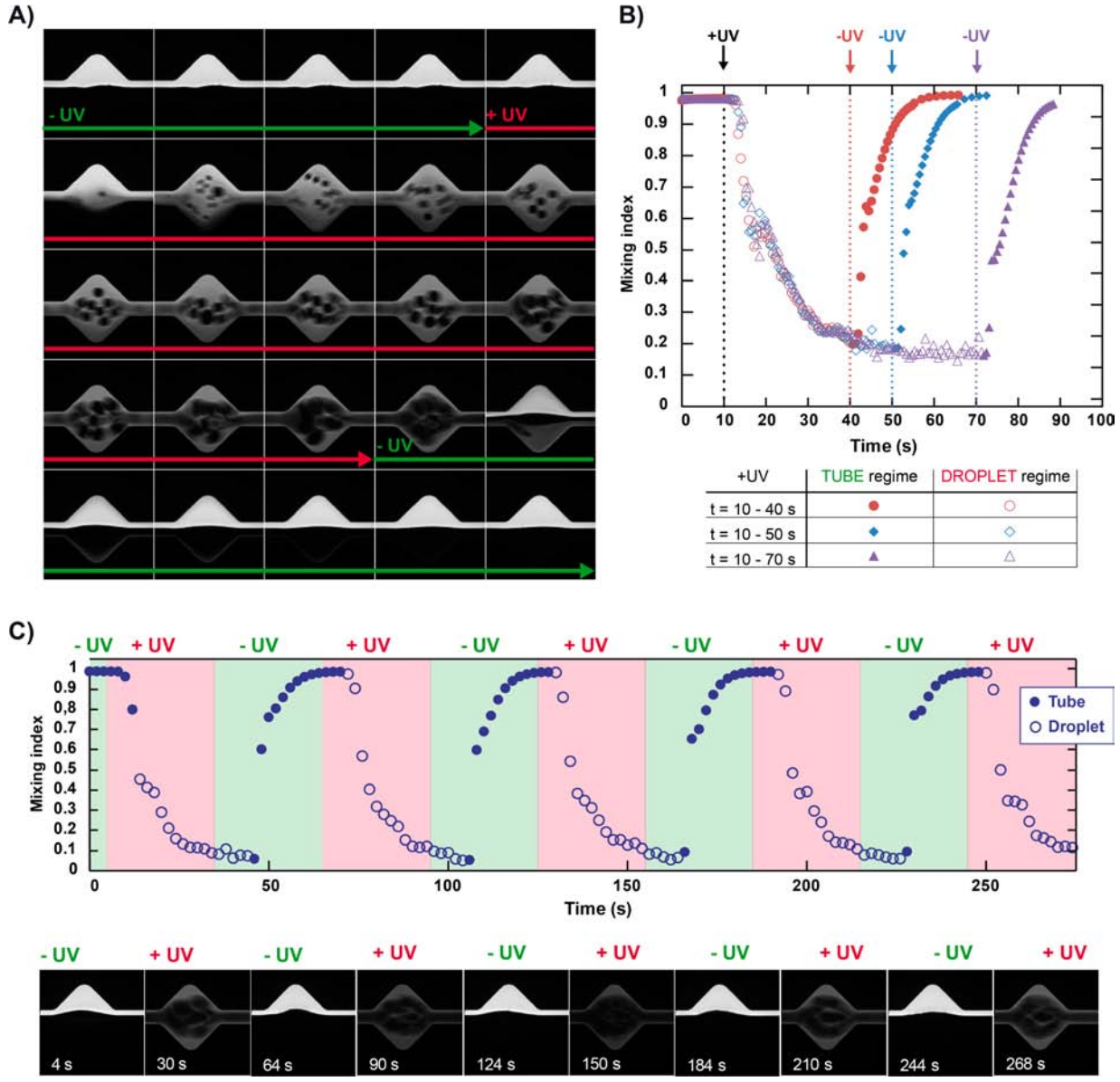

Figure 3. Dynamic behavior and reversibility in chamber 10. (A) Timelapse fluoresence microscopy images of the chamber with UV applied from t = 8.5 s to t = 38.5 s (red arrow). The first image is taken at t = 0 and images are separated by 2.16 s. Each image has a size of 768 μm × 768 μm. (B) Mixing index as a function of time for three experiments. UV is applied at 10 s for all experiments (+UV, black dashed line) and removed at 40 s (red dots), 50 s (blue diamonds) and 70 s (purple triangles). Filled and open symbols correspond to tube and droplet regimes, respectively. (C) Mixing index as a function of time (top) and fluorescence microscopy images (bottom) for successive application (+UV, red background) and removal (−UV, green background) of UV illumination. Filled and open symbols correspond to tube and droplet regimes, respectively. Q_{oil} = 0.5 μL min^{-1} (A–C); Q_{water} = 2.5 μL min^{-1} (A and B) and 3 μL min^{-1} (C); acquisition time: 10 ms (A and B) and 200 ms (C).

the intensity distributions, we calculated[42] a mixing index, MI, using the equation shown in Figure 2C where MI = 1 represents a nonmixing situation, and MI = 0 defines an ideal mixing of the oil phases. In the absence of UV, MI was almost equal to 1 in all chambers, showing the complete separation of the oil phases throughout the device. In contrast, the application of UV resulted in a marked decrease in MI with an amplitude that increased with the chamber position, from ΔMI = 0.003 ± 0.001 (chamber 1) to 0.83 ± 0.04 (chamber 10) where ΔMI was the difference in MI before and after UV (Figure 2C). These results show that the application of an external UV stimulus on our device triggers mixing of the oil phases with an efficiency that is correlated to the chamber position. As a result, it is possible to reach a target degree of mixing by adjusting the number of chambers in the device.

Role of Water Phase, Droplets and Chamber Geometry. To further define the role of the photosensitive water phase in the device, a series of control experiments were carried out. A first set of experiments was performed without the water phase. In the absence of UV, the fluorescence intensity profile around the interface was not as sharp as that in the presence of the water phase (Figure S3) showing that water in the tube regime acted as a physical separation between the two oil phases. Moreover, the mixing index values were very similar with or without water (Figure S4), which shows that efficient mixing is impossible by simply putting the oil phases into contact. These results demonstrate that droplets do not

dx.doi.org/10.1021/ja311837r | J. Am. Chem. Soc. 2013, 135, 3218−3223

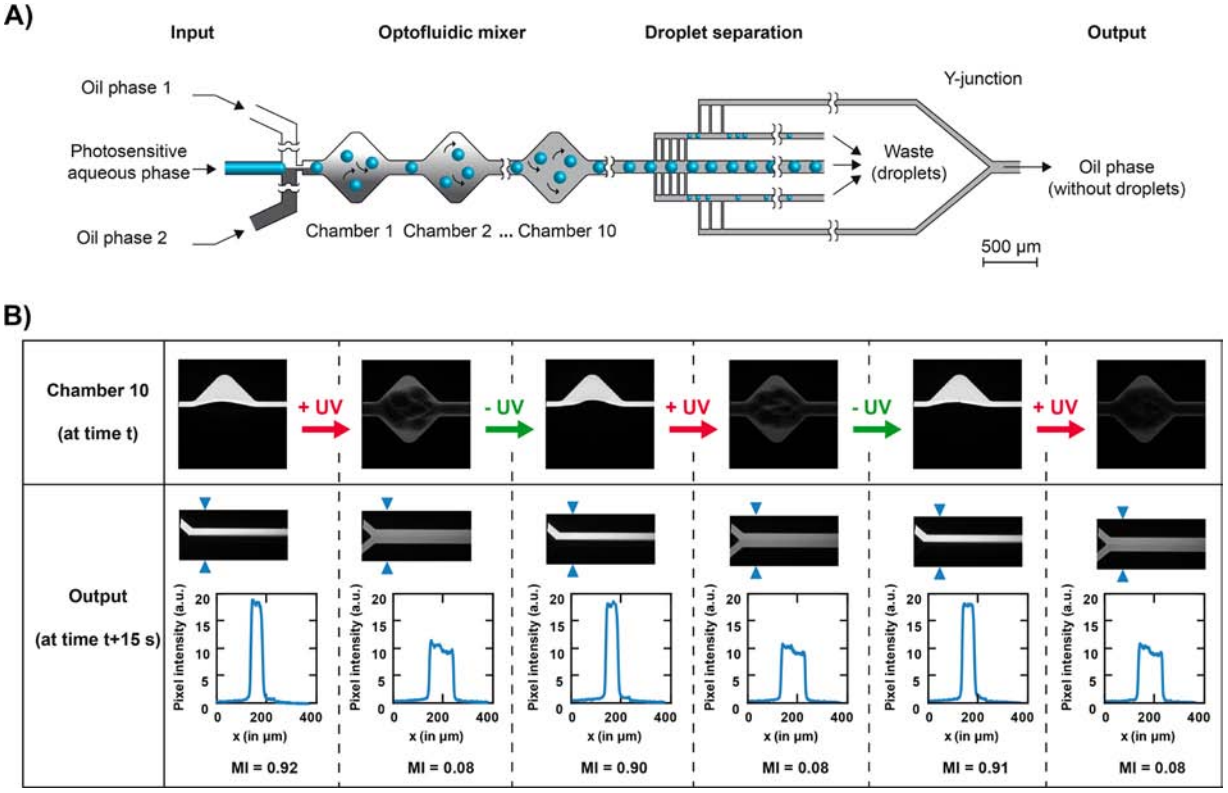

Figure 4. Optofluidic mixing after droplet removal. (A) Design (drawn to scale) of the device. (B) (Top row) Fluorescence microscopy images of chamber 10 for successive application and removal of UV illumination. Each image has a size of 768 μm × 768 μm. (Bottom row) Fluorescence microscopy images of the channel after the Y-junction taken 15 s after that of chamber 10 and intensity profiles taken between arrowheads (top to bottom). Each image has a size of 768 μm × 370 μm. Mixing index (MI) was calculated using regions adapted to the geometry (Figure S8). Q_{oil} = 0.5 μL min^{-1}; Q_{water} = 4 μL min^{-1}; acquisition time: 200 ms.

only allow oil/oil contact but also act as efficient stirrers. We also found that oil after mixing contained less than 0.3 wt % of water coming from droplets, showing a low water transfer. A second set of experiments explored the importance of droplet motion. When a channel without expansion chambers was used (Figure S5), UV illumination did induce the formation of droplets, but resulted in a mixing that was not as efficient as that seen in designs with expansion chambers, regardless of the geometry of the chambers (Figure S6). The multidirectional motion of droplets within the expansion chambers is thus crucial for extensive mixing.

Reversible Mixing. The most spectacular variation of MI upon UV illumination was observed in chamber 10 where UV triggered a transition from MI = 0.98 ± 0.02 (−UV) to MI = 0.15 ± 0.02 (+UV). The kinetics of the transition, as well as its reversibility, were therefore studied in this chamber (Figure 3). Figure 3A shows a typical timelapse observation of the mixing behavior triggered by UV. At first, in the absence of UV, the two oil phases were clearly separated. Soon after application of UV, a short transient regime was observed before the appearance of droplets in the chamber. When the UV illumination was maintained, droplets continuously stirred the two oil phases while their size tended to increase with time. Interestingly, after the UV stimulus was switched off, the water phase rapidly re-entered a stable tube regime during which the two oil phases did not mix. These results validate our approach since light can be applied as an external trigger to turn mixing on and off in a microfluidic device. We then followed the evolution of the mixing index with time for different +UV/-UV stimulations (Figure 3B). The evolution of MI after +UV was highly reproducible. The tube phase remained for only 1.2 ± 0.6 s, showing a fast response time of the droplet generation. At the exact time of droplet formation, MI started to decay, which confirms the essential role of droplets in the mixing process. In the droplet regime, MI decreased during a transition period of about 30 s to reach a stable value of MI = 0.19 ± 0.02 that could be maintained for another 30 s. When UV was turned off during the transition period, droplets were maintained for some time during which MI continued to follow the same decay. Once the tube was formed, MI rapidly increased to reach MI ≈ 1 (Figure S7). Interestingly, when UV was turned off after the transition period, the water phase re-entered the tube regime in only 0.9 ± 0.4 s followed by a sharp increase of MI up to 0.98 ± 0.01 (Figure 3B). To characterize the reversibility of the system, we applied successive −UV and +UV stimuli. Strikingly, many cycles of nonmixing/mixing behaviors could be obtained in a highly reproducible way (Figure 3C, Supporting Information Movie S2). Note that achieving such a cycling behavior required that both droplet and tube regimes remained stable over the period of the cycle. All these results establish that our setup behaves as an optofluidic mixer with several advantageous characteristics. It is fully triggered by an external light stimulus and allows repeatable and reversible switching between a nonmixing mode and an efficient mixing action.

Droplet Removal. We then investigated the possibility to remove the droplets once the required mixing was attained. This was achieved by combining the optofluidic mixer with a droplet separation unit (Figure 4A). The separation relied on two-stage comb-like structures[42] where droplets remained in the central channels while oil phases near the walls of the

dx.doi.org/10.1021/ja311837r | J. Am. Chem. Soc. 2013, 135, 3218−3223

channel could also flow in smaller lateral channels. In our device, we recovered the oil phases from the top and bottom lateral channels and combined them thanks to a Y-junction.[8] We found that 10% of the oil phase was recovered at the output, a yield that could be increased by implementing a more elaborate separation unit.[38,44−46] In this configuration, the addition of the droplet separation unit did not affect the behavior in the chamber 10 where reversible mixing was triggered by UV illumination (Figure 4B, top row). The behavior in the channel after the Y-junction (Figure 4B, bottom row) was highly correlated with that in chamber 10, with a time shift of about 15 s, which corresponded to the time needed by an element fluid to flow from chamber 10 to the output channel. Note that the water phase was efficiently removed by the droplet separation unit for the duration of the experiment. Remarkably, the intensity profiles after the Y-junction showed a succession of phase-separated behaviors and homogeneous mixing that can be obtained with a simple illumination pattern. The variation of mixing index between −UV and +UV was $\Delta MI = 0.83 \pm 0.01$ after the Y-junction, very close to the value in chamber 10. All these results show that two input oil phases injected in the device can be recovered without water as output, in a fully mixed or separated state that is controlled by light.

CONCLUSION

We described a method to reversibly control mixing in a microfluidic device using an external light stimulation provided by a portable LED device. The approach can be easily adapted to various microfluidic configurations as it does not require the implementation of any specific element (valve, electrode, etc.) inside the device. Demonstrated here with oleic acid and water, our concept might be extended to other fluids in various kinds of microdevice materials (e.g., PDMS, glass, PTFE). For each given system, it will require a proper photosensitive surfactant, which might be chosen among the library of molecules already available.[33,43,47−51] Mixing could also be performed in water phase by adapting the microfluidic substrate wetting properties to generate oil-in-water droplets. Such developments will bring the concept of optofluidic mixing described here to real world applications, such as on-demand organic or biochemical reactions in miniaturized reactors actuated by a light stimulus.

Without any laser equipment nor any elaborate optical setup, our method provides a readily portable solution for the photoactuation of microfluidic mixing. The optofluidic mixing operation described here enriches the toolbox of light-driven microfluidics[20] and constitutes a decisive step toward the realization of future all-optical fluidic chips[52] where light will fully actuate liquids in standardized and optically reconfigurable devices.

ASSOCIATED CONTENT

Supporting Information

Movies S1 and S2 (.mov files). Experimental section, supplementary figures S1−S8, and the legends of movies S1−S2. This material is available free of charge via the Internet at http://pubs.acs.org.

AUTHOR INFORMATION

Corresponding Author

damien.baigl@ens.fr

Notes

The authors declare no competing financial interest.

ACKNOWLEDGMENTS

This work was supported by the European Research Council (ERC) [European Community's Seventh Framework Programme (FP7/2007-2013) / ERC Grant agreement no. 258782], the Institut Universitaire de France (IUF), and the Mairie de Paris [Emergence(s) 2012]. A.V.-M. received a fellowship from ENS de Lyon and F.B. from ENS Cachan. We thank Y. Chen, G. Hallais and C. Tribet for experimental support; J. Fattaccioli for fruitful discussion.

REFERENCES

(1) Whitesides, G. M. *Nature* **2006**, *442*, 368−373.
(2) Nguyen, N.-T.; Wu, Z. *J. Micromech. Microeng.* **2005**, *15*, R1−R16.
(3) Mengeaud, V.; Josserand, J.; Girault, H. H. *Anal. Chem.* **2002**, *74*, 4279−4286.
(4) Wong, S.; Ward, M.; Wharton, C. *Sens. Actuators, B* **2004**, *100*, 359−379.
(5) Hong, C.; Choi, J.; Ahn, C. H. *Lab Chip* **2004**, *4*, 109−113.
(6) Xi, C.; Marks, D. L.; Parikh, D. S.; Raskin, L.; Boppart, S. A. *Proc. Natl. Acad. Sci. U.S.A.* **2004**, *101*, 7516−7521.
(7) Park, H. Y.; Kim, S. A.; Korlach, J.; Rhoades, E.; Kwok, L. W.; Zipfel, W. R.; Waxham, M. N.; Webb, W. W.; Pollack, L. *Proc. Natl. Acad. Sci. U.S.A.* **2008**, *105*, 542−547.
(8) Kamholz, A. E.; Weigl, B. H.; Finlayson, B. A.; Yager, P. *Anal. Chem.* **1999**, *71*, 5340−5347.
(9) Stroock, A. D.; Dertinger, S. K. W.; Ajdari, A.; Mezic, I.; Stone, H. A.; Whitesides, G. M. *Science* **2002**, *295*, 647−651.
(10) Niu, X.; Lee, Y. *J. Micromech. Microeng.* **2003**, *13*, 454−462.
(11) Kim, D. S.; Lee, S. W.; Kwon, T. H.; Lee, S. S. *J. Micromech. Microeng.* **2004**, *14*, 798−805.
(12) Bau, H. H.; Zhong, J.; Yi, M. *Sens. Actuators, B* **2001**, *79*, 207−215.
(13) Tsai, J.; Lin, L. *Sens. Actuators, A* **2002**, *97*−*98*, 665−671.
(14) Yang, Z.; Matsumoto, S.; Goto, H.; Matsumoto, M.; Maeda, R. *Sens. Actuators, A* **2001**, *93*, 266−272.
(15) Rife, J.; Bell, M.; Horwitz, J.; Kabler, M.; Auyeung, R. C.; Kim, W. *Sens. Actuators, A* **2000**, *86*, 135−140.
(16) Gu, W.; Zhu, X.; Futai, N.; Cho, B. S.; Takayama, S. *Proc. Natl. Acad. Sci. U.S.A.* **2004**, *101*, 15861−15866.
(17) He, B.; Burke, B. J.; Zhang, X.; Zhang, R.; Regnier, F. E. *Anal. Chem.* **2001**, *73*, 1942−1947.
(18) Johnson, T. J.; Ross, D.; Locascio, L. E. *Anal. Chem.* **2002**, *74*, 45−51.
(19) Psaltis, D.; Quake, S. R.; Yang, C. *Nature* **2006**, *442*, 381−386.
(20) Baigl, D. *Lab Chip* **2012**, *12*, 3637−3653.
(21) Liu, G. L.; Kim, J.; Lu, Y.; Lee, L. P. *Nat. Mater.* **2006**, *5*, 27−32.
(22) Terray, A.; Oakey, J.; Marr, D. W. M. *Science* **2002**, *296*, 1841−1844.
(23) Ladavac, K.; Grier, D. *Opt. Express* **2004**, *12*, 1144−1149.
(24) Neale, S. L.; MacDonald, M. P.; Dholakia, K.; Krauss, T. F. *Nat. Mater.* **2005**, *4*, 530−533.
(25) Di Leonardo, R.; Leach, J.; Mushfique, H.; Cooper, J.; Ruocco, G.; Padgett, M. *Phys. Rev. Lett.* **2006**, *96*, 134502.
(26) Zhang, K.; Jian, A.; Zhang, X.; Wang, Y.; Li, Z.; Tam, H.-Y. *Lab Chip* **2011**, *11*, 1389−1395.
(27) Moorthy, J.; Khoury, C.; Moore, J. S.; Beebe, D. J. *Sens. Actuators, B* **2001**, *75*, 223−229.
(28) Diguet, A.; Li, H.; Queyriaux, N.; Chen, Y.; Baigl, D. *Lab Chip* **2011**, *11*, 2666−2669.
(29) Park, S.-Y.; Wu, T.-H.; Chen, Y.; Teitell, M. A.; Chiou, P.-Y. *Lab Chip* **2011**, *11*, 1010−1012.
(30) Chiou, P. Y.; Moon, H.; Toshiyoshi, H.; Kim, C.-J.; Wu, M. C. *Sens. Actuators, A* **2003**, *104*, 222−228.
(31) Chiou, P. Y.; Ohta, A. T.; Wu, M. C. *Nature* **2005**, *436*, 370−372.

(32) Kotz, K. T.; Noble, K. A.; Faris, G. W. *Appl. Phys. Lett.* **2004**, *85*, 2658.
(33) Diguet, A.; Guillermic, R.-M.; Magome, N.; Saint-Jalmes, A.; Chen, Y.; Yoshikawa, K.; Baigl, D. *Angew. Chem., Int. Ed.* **2009**, *48*, 9281−9284.
(34) Delville, J.-P.; Robert de Saint Vincent, M.; Schroll, R. D.; Chraïbi, H.; Issenmann, B.; Wunenburger, R.; Lasseux, D.; Zhang, W. W.; Brasselet, E. *J. Opt. A: Pure Appl. Opt.* **2009**, *11*, 034015.
(35) Hellman, A. N.; Rau, K. R.; Yoon, H. H.; Bae, S.; Palmer, J. F.; Phillips, K. S.; Allbritton, N. L.; Venugopalan, V. *Anal. Chem.* **2007**, *79*, 4484−4492.
(36) Tice, J. D.; Song, H.; Lyon, A. D.; Ismagilov, R. F. *Langmuir* **2003**, *19*, 9127−9133.
(37) Song, H.; Chen, D. L.; Ismagilov, R. F. *Angew. Chem., Int. Ed.* **2006**, *45*, 7336−7356.
(38) Teh, S.-Y.; Lin, R.; Hung, L.-H.; Lee, A. P. *Lab Chip* **2008**, *8*, 198−220.
(39) Günther, A.; Khan, S. A.; Thalmann, M.; Trachsel, F.; Jensen, K. F. *Lab Chip* **2004**, *4*, 278−286.
(40) Garstecki, P.; Fuerstman, J.; M.; Fischbach, M. A.; Sia, S. K.; Whitesides, G. M. *Lab Chip* **2006**, *6*, 207−212.
(41) Wang, S. S.; Jiao, Z. J.; Huang, X. Y.; Yang, C.; Nguyen, N. T. *Microfluid. Nanofluid.* **2008**, *6*, 847−852.
(42) Mao, X.; Juluri, B. K.; Lapsley, M. I.; Stratton, Z. S.; Huang, T. J. *Microfluid. Nanofluid.* **2009**, *8*, 139−144.
(43) Diguet, A.; Mani, N. K.; Geoffroy, M.; Sollogoub, M.; Baigl, D. *Chem.–Eur. J.* **2010**, *16*, 11890−11896.
(44) Angelescu, D. E.; Mercier, B.; Siess, D.; Schroeder, R. *Anal. Chem.* **2010**, *82*, 2412−2420.
(45) Huh, D.; Bahng, J. H.; Ling, Y.; Wei, H.; Kripfgans, O. D.; Fowlkes, J. B.; Grotberg, J. B.; Takayama, S. *Anal. Chem.* **2007**, *79*, 1369−1376.
(46) Kralj, J. G.; Schmidt, M. A.; Jensen, K. F. *Lab Chip* **2005**, *5*, 531−535.
(47) Shin, J. Y.; Abbott, N. L. *Langmuir* **1999**, *15*, 4404−4410.
(48) Liu, X.; Abbott, N. L. *J. Colloid Interface Sci.* **2009**, *339*, 1−18.
(49) Eastoe, J.; Sanchez-Dominguez, M.; Cumber, H.; Burnett, G.; Wyatt, P.; Heenan, R. K. *Langmuir* **2003**, *19*, 6579−6581.
(50) Chevallier, E.; Mamane, A.; Stone, H. A.; Tribet, C.; Lequeux, F.; Monteux, C. *Soft Matter* **2011**, *7*, 7866.
(51) Chevallier, E.; Monteux, C.; Lequeux, F.; Tribet, C. *Langmuir* **2012**, *28*, 2308−2312.
(52) Glückstad, J. *Nat. Mater.* **2004**, *3*, 9−10.